

A soluble activin receptor Type IIA fusion protein (ACE-011) increases bone mass via a dual anabolic-antiresorptive effect in Cynomolgus monkeys

Sutada Lotinun^{a,*}, R. Scott Pearsall^b, Monique V. Davies^b, Tod H. Marvell^b, Travis E. Monnell^b, Jeffrey Ucran^b, Roberto J. Fajardo^{c,1}, Ravindra Kumar^b, Kathryn W. Underwood^b, Jasbir Seehra^b, Mary L. Bouxsein^c, Roland Baron^{a,d}

^a Department of Oral Medicine, Infection and Immunity, Harvard School of Dental Medicine, Boston, MA 02115, USA

^b Acceleron Pharma, Inc., 149 Sidney Street, Cambridge, MA 02139, USA

^c Orthopedic Biomechanics Laboratory, Beth Israel Deaconess Medical Center and Harvard Medical School, Boston, MA 02215, USA

^d Endocrine Unit, Massachusetts General Hospital and Harvard Medical School, Boston, MA 02114, USA

ARTICLE INFO

Article history:

Received 26 April 2009

Revised 16 December 2009

Accepted 9 January 2010

Available online 18 January 2010

Edited by: Robert Recker

Keywords:

Activin A

ActRIIA

Osteoporosis

Osteoblast

Osteoclast

ABSTRACT

Activin A belongs to the TGF- β superfamily and plays an important role in bone metabolism. It was reported that a soluble form of extracellular domain of the activin receptor type IIA (ActRIIA) fused to the Fc domain of murine IgG, an activin antagonist, has an anabolic effect on bone in intact and ovariectomized mice. The present study was designed to examine the skeletal effect of human ActRIIA-IgG1-Fc (ACE-011) in non-human primates. Young adult female Cynomolgus monkeys were given a biweekly subcutaneous injection of either 10 mg/kg ACE-011 or vehicle (VEH) for 3 months. Treatment effects were evaluated by histomorphometric analysis of the distal femur, femoral midshaft, femoral neck and 12th thoracic vertebrae, by μ CT analysis of femoral neck and by biomarkers of bone turnover. Compared to VEH, at the distal femur ACE-011-treated monkeys had significantly increased cancellous bone volume (+93%), bone formation rate per bone surface (+166%) and osteoblast surface (+196%) indicating an anabolic action. Monkeys treated with ACE-011 also had decreased osteoclast surface and number. No differences were observed in parameters of cortical bone at the midshaft of the femur. Similar to distal femur, ACE-011-treated monkeys had significantly greater cancellous bone volume, bone formation rate and osteoblast surface at the femoral neck relative to VEH. A significant increase in bone formation rate and osteoblast surface with a decrease in osteoclast surface was observed in thoracic vertebrae. μ CT analysis of femoral neck indicated more plate-like structure in ACE-011-treated monkeys. Monkeys treated with ACE-011 had no effect on serum bone-specific alkaline phosphatase and CTX at the end of the study. These observations demonstrate that ACE-011 is a dual anabolic-antiresorptive compound, improving cancellous bone volume by promoting bone formation and inhibiting bone resorption in non-human primates. Thus, soluble ActRIIA fusion protein may be useful in the prevention and/or treatment of osteoporosis and other diseases involving accelerated bone loss.

© 2010 Elsevier Inc. All rights reserved.

Introduction

Most of the drugs approved for the prevention and treatment of osteoporosis (i.e. selective estrogen modulators, bisphosphonates and calcitonin) act by inhibiting bone resorption and thereby preventing further bone loss [1]. They do not stimulate new bone formation, and thus fail to reverse prior bone loss. In contrast, parathyroid hormone (PTH), the only FDA-approved anabolic agent, increases bone remodeling and improves bone mass and microarchitecture [2]. However, PTH has adverse effects, including nausea, dizziness, headache,

hypercalcemia and hypercalciuria and can be prescribed for only two years in the US [2,3]. Until now, there are no FDA-approved drugs that play dual role in inhibiting bone resorption and also stimulating bone formation. Thus, there is a clear clinical need to develop anabolic-antiresorptive compounds since targeting both osteoblasts and osteoclasts might be the most effective therapeutic approach to reverse osteoporosis.

Activins are multifunctional proteins that belong to the TGF- β superfamily and are composed of four different β -subunits (β A, β B, β C and β E) [4,5]. Homo- and heterodimerization of β A and β B subunits gives rise to three biologically active glycoproteins, including activin A (β A- β A), activin B (β B- β B) and activin AB (β A- β B). Activins mediate their signal transduction cascades through serine-threonine kinase receptors, including the type I receptors, comprising the activin receptor-like kinase 2 (ALK2) and 4 (ALK4), and the type II receptors,

* Corresponding author. Fax: +1 617 432 1897.

E-mail address: sutada_lotinun@hsdm.harvard.edu (S. Lotinun).

¹ Current address: Department of Orthopaedics, University of Texas Health Science Center at San Antonio, San Antonio, TX 78229, USA.

comprising the activin type IIA (ActRIIA) and type IIB (ActRIIB) [6–8]. Activins bind with high affinity to ActRIIA or ActRIIB receptors leading to the recruitment and phosphorylation of ALK4 followed by activation of intracellular signaling molecules, Smad 2 and 3 [9].

Mice with a mutation in the gene encoding the activin β A subunit have development-related defects in their secondary palates and die within 24 h of birth while mice deficient in activin β B are viable, indicating a crucial role of activin β A in craniofacial development [10]. Activin A is abundantly localized in extracellular bone matrix but its precise role in bone homeostasis is controversial. It has been shown that activin A enhances the induction of ectopic bone formation when implanted concurrently with BMPs [11], increases osteoblast proliferation and collagen synthesis [12] and stimulates fracture healing [13]. Local injection of activin A onto the periosteum of parietal bone in newborn rats increases the thickness of periosteum and bone matrix layers [14]. However, several studies demonstrated an inhibitory effect of activin A on osteoblast differentiation in murine, rat, and human *in vitro* [15–17]. Additionally, activin A stimulates osteoclastogenesis *in vitro* whereas inhibin exhibits an opposite effect [18]. It has been recently reported that an activin antagonist, the soluble extracellular domain of ActRIIA fused to a murine IgG2a-Fc (ActRIIA-mFc), stimulates bone formation, resulting in increased bone mass and strength in intact and ovariectomized (OVX) mice [19]. In addition, ActRIIA-mFc decreases osteoclast surface after 2 weeks of treatment in 12-week-old mice.

The purpose of the present study was to extend previous work by testing a human ActRIIA-IgG1-Fc fusion protein (ACE-011, Fig. 1) in non-human primates. We addressed the following questions: (1) does ACE-011 increase cancellous bone volume in Cynomolgus monkeys, a species in which bone remodeling is similar to that in humans; (2) if so, is increased bone volume due to an increase in bone formation, a decrease in bone resorption or both; (3) does ACE-011 alter cortical bone mass; and (4) what impact does ACE-011 have on biomarkers of bone turnover? The skeletal actions of ACE-011 were determined using bone histomorphometry, μ CT and serum markers of bone metabolism. Our findings indicate that biweekly treatment with 10 mg/kg ACE-011 for 3 months is well-tolerated and acts as anabolic and antiresorptive agent, increasing cancellous bone mass at various sites in Cynomolgus monkeys.

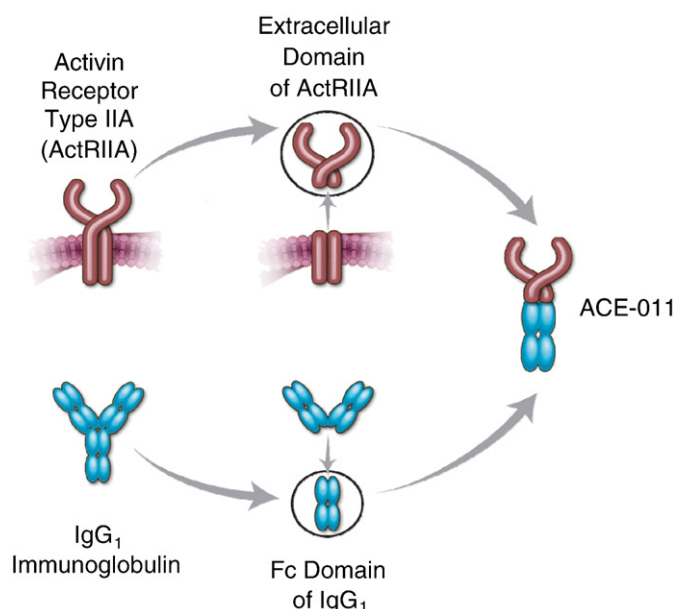


Fig. 1. A schematic diagram of human fusion protein of the extracellular domain of ActRIIA and the Fc domain of IgG₁ (ACE-011).

Materials and methods

Study design

Young adult female Cynomolgus monkeys (*Macaca fascicularis*, $n=11$) were quarantined and acclimated to laboratory conditions for 30 days prior to release to a stock colony (Bridge Laboratories, Maryland). Animals from the stock colony were transferred to an experimental room and housed individually in stainless steel cages for 7 days prior to experiments. They were fed fresh food twice daily (Certified Global Harlan Teklad Laboratory 2055C Primate Diet) and provided water *ad libitum*. The study room was maintained at 18 to 29 °C, with a humidity range of 30 to 70%, under a 12-h light, 12-h dark cycle. Animals were provided with environmental enrichment consisting of visual contact with other non-human primates, food puzzles (at least three times a week) and/or rubber toys that remained in the cage. Additionally, fruit and/or other primate treats were given to the animals periodically throughout the study. All animal experiments were conducted in accordance with the Institutional Animal Care and Use Committee and in accordance with provisions of the USDA Animal Welfare Act, the PHS Policy on Humane Care and Use of Laboratory Animals, and the US Interagency Research Animal Committee Principles for the Utilization and Care of Research Animals.

Following acclimatization, eleven monkeys were randomly divided into vehicle- (VEH, $n=5$) and ACE-011-treated group ($n=6$). A prior pharmacokinetic study indicated that a single subcutaneous injection of 1, 10 and 30 mg/kg body weight ACE-011 dose dependently increases serum ACE-011 concentration with an elimination half-life of 7–9 days (20). Therefore, ACE-011 was administered biweekly to determine the skeletal effects and the 10 mg/kg dose was chosen as an efficacious dose in this animal model.

The monkeys were injected subcutaneous with either PBS (VEH) or ACE-011 (10 mg/kg body weight) every 14 days for 3 months. Cageside observations for mortality, moribundity, general health and signs of toxicity were conducted daily. Clinical observations included evaluation of skin and fur characteristics, injection site, eye and mucous membranes, respiratory, circulatory, autonomic and central nervous systems. Daily qualitative food consumption was evaluated. Blood samples were collected after an overnight fast from the femoral vein into serum separator tubes on days 1 (baseline), 15, 29, 43, 57, 71, 85 and 92 of treatment for determination of serum biomarkers of bone turnover, including bone alkaline phosphatase (ALP) and C-terminal telopeptide of type I collagen (CTX).

Following VEH or ACE-011 administration on study day 71, all animals were administered tetracycline (30 mg/kg) by an intravenous infusion pump (12.6 ml/kg/h) through a saphenous vein using an Advanced 1200 series infusion pump. On study day 85, all animals were administered calcein (1 mg/kg) as a slow bolus (3 to 5 min) intravenous injection through a saphenous vein. The animals were euthanized via an intravenous dose of sodium pentobarbital followed by exsanguination on study day 92. The left femurs and 12th thoracic vertebrae were removed, cleared of adherent tissues and fixed in 70% alcohol.

Cancellous bone histomorphometry

Histomorphometry was used to examine changes in cancellous bone architecture at three different sites, including distal femur, femoral neck and 12th thoracic vertebra. The 3.5-cm-long distal femurs were cut using low-speed diamond-edge saw (Isomet Plus, Buehler, Lake Bluff, IL, USA) and the cortical bone of ventral femurs were trimmed off to expose distal metaphysis to 70% ethanol. The distal femur was embedded in methyl methacrylate (Polysciences, Warrington, PA) with condyle head down. For the femoral neck, the proximal femurs were clamped in the chuck of low-speed diamond-

edge saw and femoral head and neck were cut from the shaft. Most of the femoral head was removed using a grinder-polisher (Phoenix Alpha and Beta Grinder-Polishers, Buehler, Lake Bluff, IL, USA). The femoral neck was then fixed in 70% ethanol and embedded in methyl methacrylate, with the femoral head end down. After necropsy, the 12th thoracic vertebrae were cut sagittally and transverse processes were removed. The left side of the vertebral body was processed for histomorphometric analysis.

Distal femur, femoral neck and vertebra were dehydrated in ethanol, infiltrated, and embedded without demineralization in methyl methacrylate. Undecalcified longitudinal sections of the distal femur metaphysis (8 μm thick) were cut with Jung Polycut E microtome (Leica, Heidelberg, Germany) and mounted unstained for dynamic measurements. Consecutive sections were cut at 5 μm thickness and toluidine blue stained to quantitate bone cell measurements. The vertebra and femoral neck sections were cut on a Leica RM 2165 microtome (Heidelberg, Germany). All histomorphometric indices were measured at 25 \times objective and area of each field is approximately 0.16 mm². A sampling site of 10 fields \times 7 fields was established in the secondary spongiosa of the distal metaphysis of femur. The femoral neck was oriented and measurements were made in the cancellous region comprising 9 fields \times 7 fields located centrally in the section. Vertebral measurements were made 0.8 mm below the growth plate comprising 14 fields \times 5 fields. Histomorphometric parameters were carried out semiautomatically using OsteoMeasure image analyzer (OsteoMetric Inc., Atlanta, GA) and expressed according to standardized nomenclature [21]. The following measurements were obtained: bone volume per tissue volume (BV/TV, %), trabecular thickness (Tb.Th, μm), trabecular separation (Tb.Sp, μm) and trabecular number (Tb.N, /mm). Mineralizing surface per bone surface (MS/BS, %) was defined as the percentage of double-labeled plus 1/2 single-labeled surface. Mineral apposition rate (MAR, $\mu\text{m}/\text{day}$) was defined as the mean distance between the fluorescent labels divided by the interval of 14 days. Bone formation rate was calculated as the product of MS/BS and MAR and expressed per bone surface referent (BFR/BS, $\mu\text{m}^3/\mu\text{m}^2/\text{year}$), bone volume referent (BFR/BV, %/year) and tissue volume referent (BFR/TV, %/year). Osteoblast surface (Ob.S/BS, %) and osteoclast surface (Oc.S/BS, %) were determined as trabecular surface covered by large basophilic cuboidal cells and multinucleated (2 or more nuclei) cells in toluidine blue stained sections, respectively. Osteoblast number (N.Ob/BPm, /mm) and osteoclast number (N.Oc/BPm, /mm) were counted and expressed per bone perimeter. Osteoid surface (OS/BS, %), osteoid thickness (O.Th, μm) and eroded surface (ES/BS, %) were measured.

Cortical bone histomorphometry

Cross-sections (150 μm thick) obtained from midshaft of the left femur using low-speed diamond-edge saw were ground on a grinder-polisher to approximately 20 μm thick and mounted unstained. Cross-sectional area (CSA, mm²), cortical area (CA, mm²), medullary area (MA, mm²), periosteal perimeter (mm) and endocortical perimeter (mm) were measured at 2.5 \times objective.

μCT analysis

A high-resolution desktop micro-tomographic imaging system ($\mu\text{CT}40$, Scanco Medical AG, Brüttisellen, Switzerland) was used to assess trabecular bone microarchitecture in the mid-femoral neck region adjacent to where the histomorphometric sections were taken. Specimens were embedded in plastic. Scans were acquired over 1 mm using a 20 μm isotropic voxel size, 70 kVp and 114 mAs, and were subjected to Gaussian filtration. A cylindrical volume of interest (height = 1 mm, diameter = 4 to 6 mm, depending on size of femoral neck) including only trabecular bone was identified for each specimen. Images were segmented using an adaptive-iterative algorithm

and morphometric variables were computed from the binarized images using direct, 3D techniques. We assessed bone volume fraction (BV/TV, %), trabecular thickness (Tb.Th, μm), trabecular number (Tb.N, /mm), trabecular separation (Tb.Sp, μm), connectivity density (ConnD, /mm³), and structure model index (SMI), which describes the plate-vs-rod-like nature of the architecture.

Serum analyses

Serum bone-specific ALP

The Ostase assays were performed with the Access Immunoassay System™ (Beckman Coulter) which provides a quantitative measurement of bone ALP. The Access Ostase assay is a one-step immunoenzymatic assay.

Serum CTX

These assays were performed with the Serum Crosslaps® kit from Nordic Bioscience (Herlev, Denmark) which is an enzyme immunoassay kit for the quantitative determination of a type 1 collagen specific sequence in serum.

Statistical analysis

Results are expressed as mean \pm SEM. Because of the small sample size in this study, differences between groups were compared using a non-parametric Mann–Whitney *U* test. Measurements at $p < 0.05$ (one-tailed) were considered to be statistically significant. The non-parametric statistical analyses were performed with GraphPad Prism version 4.0. Dixon's *Q*-test was used for testing and removing an outlier in control group.

Results

Based on previous findings that the pharmacological blockade of activin signaling through the ActRIIA receptor has skeletal anabolic effect in mice, it was of interest to further examine the effects of activin antagonist on bone turnover in non-human primates. Biweekly subcutaneous dosing of 10 mg/kg ACE-011 was generally well tolerated. No treatment-related changes in clinical observation were reported over 3-month period. However, there was an incidence of diarrhea in one monkey on study days 18, 70, 71, 76 and 77 leading to withdrawal of this monkey from ACE-011-treated group. Gross pathology revealed no visible lesion in gastrointestinal tract and the illness was not considered test article related. In addition, one outlier was found in controls and all data from this animal were eliminated from the group mean.

ACE-011 stimulated bone formation and inhibited bone resorption in cancellous bone

Table 1 summarizes the cancellous histomorphometric findings at distal femur, femoral neck and 12th thoracic vertebra. Compared to VEH, ACE-011 significantly increased cancellous bone volume by 93% with a 42% increase in trabecular thickness, 39% increase in trabecular number and 51% decrease in trabecular separation at the distal femur metaphysis. Bone formation rate was substantially increased in ACE-011-treated monkeys, due to significant increases in both mineralizing surface and mineral apposition rate. Osteoblast surface and osteoblast number were increased by a factor of 3 in monkeys treated with ACE-011. In addition, ACE-011 suppressed indices of bone resorption, including osteoclast surface, osteoclast number and eroded surface. Similar to the distal femur, ACE-011 treatment led to an increase in cancellous bone volume at the femoral neck relative to VEH. The increase in bone volume was associated with increased indices of bone formation such as mineralizing surface, mineral apposition rate, bone formation rate expressed per bone surface

Table 1
Effects of ACE-011 on cancellous bone histomorphometry at three different sites.

Parameters	Distal femur		Femoral neck		Thoracic vertebra	
	VEH	ACE-011	VEH	ACE-011	VEH	ACE-011
	(n = 4)	(n = 5)	(n = 4)	(n = 5)	(n = 4)	(n = 5)
BV/TV (%)	22.01 ± 3.64	42.47 ± 1.90*	40.77 ± 3.82	53.81 ± 3.53*	26.77 ± 3.84	31.88 ± 1.40
Tb.Th (µm)	137 ± 10	194 ± 11*	176 ± 13	211 ± 26	120.25 ± 10.39	122.26 ± 6.60
Tb.N (/mm)	1.58 ± 0.19	2.20 ± 0.07*	2.30 ± 0.09	2.66 ± 0.28	2.20 ± 0.15	2.62 ± 0.10*
Tb.Sp (µm)	532 ± 106	262 ± 13*	259 ± 23	186 ± 32	342 ± 44	261 ± 12*
MS/BS (%)	11.95 ± 0.98	20.58 ± 2.61*	9.22 ± 2.77	16.47 ± 0.58*	7.99 ± 1.34	15.89 ± 3.04*
MAR (µm/day)	1.04 ± 0.07	1.58 ± 0.04*	0.81 ± 0.05	1.10 ± 0.10*	1.09 ± 0.11	0.96 ± 0.08
BFR/BS (µm ³ /µm ² /year)	45.05 ± 3.45	120.01 ± 17.86*	28.00 ± 9.04	66.21 ± 6.62*	32.91 ± 7.97	55.37 ± 11.25
BFR/BV (%/year)	64.90 ± 4.59	144.72 ± 32.69*	34.14 ± 13.71	70.16 ± 9.91	55.63 ± 15.02	90.99 ± 17.54
BFR/TV (%/year)	16.07 ± 2.65	59.82 ± 11.61*	12.42 ± 3.80	35.92 ± 5.76*	14.02 ± 2.89	28.47 ± 4.83*
N.Ob/BPm (/mm)	3.55 ± 0.37	10.46 ± 0.88*	1.00 ± 0.58	3.22 ± 0.84	2.55 ± 0.82	4.55 ± 0.61
Ob.S/BS (%)	6.72 ± 0.60	19.87 ± 1.81*	1.52 ± 0.77	4.87 ± 1.06*	3.50 ± 1.02	6.82 ± 0.95*
OS/BS (%)	22.53 ± 4.34	28.94 ± 1.14	8.71 ± 5.41	11.46 ± 3.62	11.77 ± 2.99	13.62 ± 3.86
O.Th (µm)	11.84 ± 0.66	14.15 ± 0.55*	8.89 ± 0.76	9.91 ± 0.52	11.85 ± 1.63	9.54 ± 0.24
N.Oc/BPm (/mm)	0.58 ± 0.19	0.25 ± 0.04*	0.24 ± 0.09	0.32 ± 0.09	0.21 ± 0.05	0.11 ± 0.03
Oc.S/BS (%)	3.72 ± 0.39	1.57 ± 0.26*	1.66 ± 0.66	2.06 ± 0.57	1.16 ± 0.28	0.46 ± 0.12*
ES/BS (%)	7.05 ± 0.28	4.46 ± 1.04*	2.74 ± 0.70	2.25 ± 0.15	2.43 ± 0.11	0.77 ± 0.17*

Results are mean ± SEM. **p* < 0.05 compared to vehicle.

referent and tissue volume referent and osteoblast surface. However, osteoclast surface and osteoclast number were similar in VEH- and ACE-011-treated animals. Fig. 2 shows representative images of distal femur and femoral neck in VEH- and ACE-011-treated monkeys. In thoracic vertebrae, monkey treated with ACE-011 exhibited a non-significant increased cancellous bone volume compared to VEH-treated monkey. However, bone formation rate was significantly increased when expressed per tissue volume referent. The increase in bone formation rate resulted in a 19% increase in trabecular number and a 24% decrease in trabecular separation. Treatment with ACE-011 increased osteoblast surface and decreased osteoclast surface and eroded surface relative to VEH controls.

ACE-011 had no effect on cortical bone histomorphometry

The effects of ACE-011 on cortical bone histomorphometry at femur midshaft are shown in Table 2. There were no differences in cross-sectional area, cortical area, marrow area, periosteal perimeter and endocortical perimeter between VEH- and ACE-011-treated monkeys. A 14-day interlabel interval was not sufficient to separate the two fluorochrome labels at periosteum and endocortical bone, preventing the measurement of mineral apposition rate.

ACE-011 changed structure model type toward plate-like architecture

µCT analysis of femoral neck is summarized in Table 3. Monkeys treated with ACE-011 had slightly higher cancellous bone volume (*p* = 0.095) and significantly lower (i.e., more plate-like) SMI (*p* = 0.032, Fig. 3). The structure model type changed toward more plate-like in ACE-011-treated monkeys (Fig. 3). Tb.Th, Tb.N, Tb.Sp and Conn.D did not differ significantly between VEH- and ACE-011-treated monkeys.

ACE-011 had no effect on serum bone-specific ALP and CTX levels

Serum levels of bone formation marker ALP and bone resorption marker CTX in the VEH and ACE-011 group were similar on day 1. Serum ALP levels showed a trend for an increase at study days 15 and 29 (36–40%), but returned to near baseline levels by the end of the study (day 92). At the end of the study, there was no change in serum bone-specific ALP in VEH- and ACE-011-treated monkeys (99.69 ± 44.51 vs 126.73 ± 22.38 ng/ml). These transient early changes in bone ALP are consistent with those seen in a Phase I study in human

patients (22). CTX levels did not differ between VEH and ACE-011 group at the end of the study (1.78 ± 0.59 vs 1.86 ± 0.39 ng/ml).

Discussion

The present study investigates the skeletal effects of soluble ActRIIA fusion protein ACE-011 in non-human primates. Treatment with 10 mg/kg ACE-011 every 14 days for 3 months was well-tolerated and not associated with any serious adverse events. ACE-011 had a positive effect on cancellous bone mass and architecture primarily at appendicular sites whereas the midshaft diaphyseal femur, an ideal site for the analysis of cortical bone in non-human primates, remained relatively unchanged. The increased cancellous bone volume in ACE-011-treated monkey was due to a marked increase in bone formation accompanied by either a modest decrease or no change in bone resorption.

The histomorphometric results reported here confirm previous findings that the inhibition of activin signaling through the ActRIIA receptor has anabolic effect in mice [19]. Cancellous bone formation rate when expressed per tissue volume was increased at distal femur, femoral neck and thoracic vertebra following administration of ACE-011. The increase in bone formation rate led to increased cancellous bone volume. µCT analysis of femoral neck indicated more plate-like trabecular structure in ACE-011-treated monkeys. Although changes in cancellous bone volume at thoracic vertebra were not statistically significant, the magnitude of increase was 19%. The lack of statistical significance may be related to low sample size in these studies, or the use of a human Fc molecule in monkeys which may elicit an antibody response by the monkeys leading to increased clearance or reduced bioactivity of the drug in a repeat dosing setting. Serum bone-specific ALP, a marker of bone formation, was no significant change after 3 months of ACE-011 treatment. Other studies in monkeys have shown variable responsiveness of bone biomarkers to increased bone formation associated with anabolic agents [23,24]. The variable results could be due to different responses in cortical and cancellous bone or related to the mechanism of action of different compounds. However, longer-term studies would be necessary to detect the effects of ACE-011 on bone turnover markers. A compression test of 5th lumbar vertebra indicated that ACE-011 increased stiffness, yield force and work to failure [20]. These findings suggest that the soluble ActRIIA fusion protein ACE-011 improve mechanical properties.

The actions of ACE-011 may parallel the role of follistatin, an endogenous soluble protein which binds multiple TGF-β ligands,

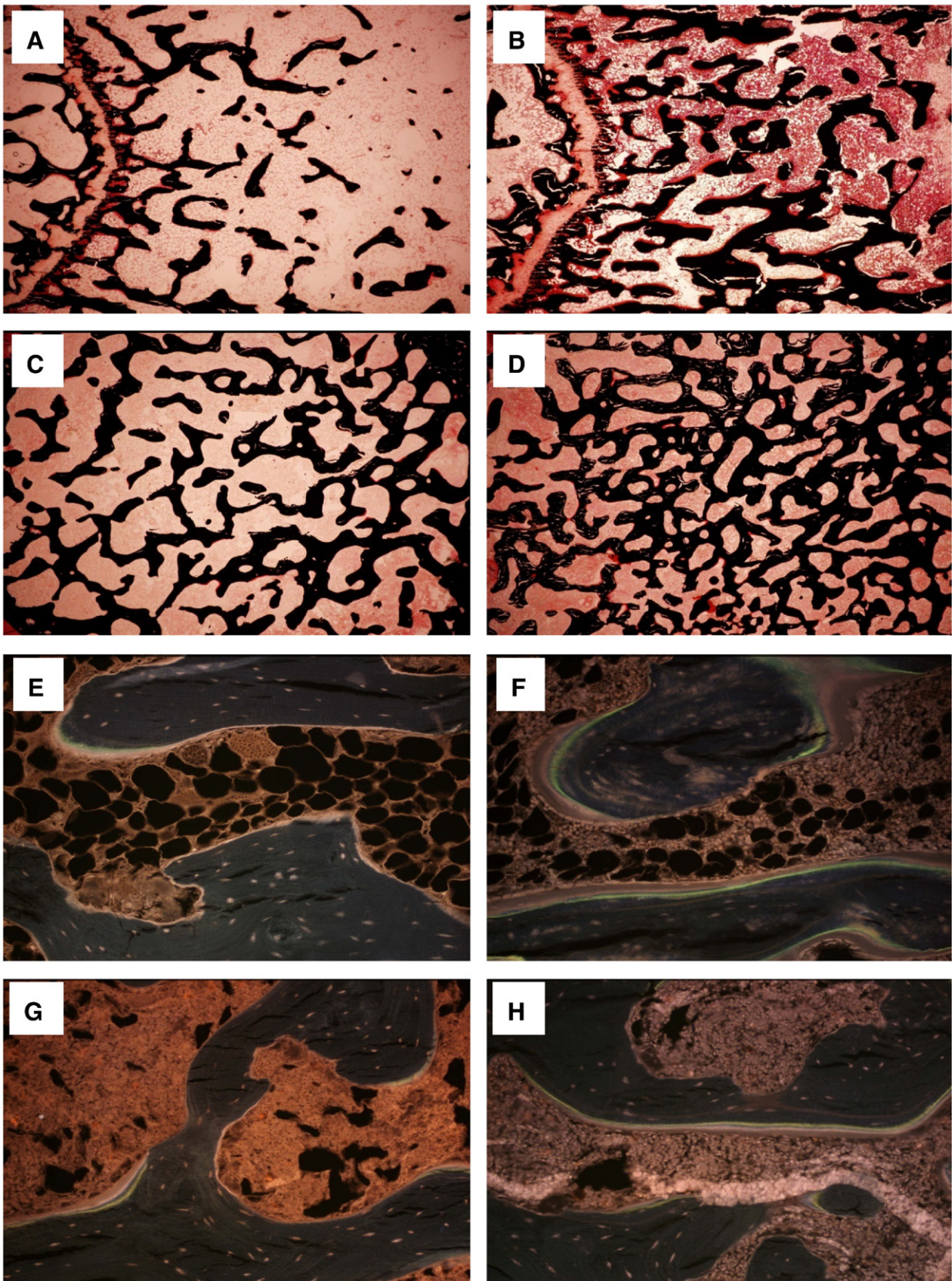


Fig. 2. Representative photomicrographs showing Von Kossa's stain and fluorescent sections from distal femur metaphysis in Cynomolgus monkeys treated with VEH (A, E) and ACE-011 (B, F) and femoral neck in Cynomolgus monkeys treated with VEH (C, G) and ACE-011 (D, H), respectively.

Table 2
Effects of ACE-011 on static cortical bone histomorphometric measurements at midshaft femur.

Parameters	VEH	ACE-011
	(n = 4)	(n = 5)
CSA (mm ²)	66.09 ± 4.83	65.81 ± 2.73
CA (mm ²)	41.76 ± 2.83	46.41 ± 2.77
MA (mm ²)	24.33 ± 3.97	19.39 ± 1.85
Periosteal Perimeter (mm)	30.66 ± 1.70	29.66 ± 0.65
Endocortical Perimeter (mm)	18.11 ± 1.60	15.96 ± 0.77

Results are mean ± SEM. CSA, cross-sectional area; CA, cortical area; MA, marrow area.

including activin, and prevents them from interacting with their receptors [25]. Follistatin is expressed locally in most of tissues that also express activin [26–30], including muscle, brain, kidney, salivary gland, liver, adrenal gland, ovary, testis and bone, but is not found at high levels in circulation, indicating that it may act in a paracrine manner to block ligand signaling. In bone cells, follistatin transcript is detected in osteoblasts [30], osteocytes [30] and MC3T3-E1 cells [31]. The extent of mineralization may be regulated by the ratio of activin A-to-follistatin in mature osteoblasts [17]. In vitro, neutralization of endogenous activins by follistatin increases matrix mineralization through mechanisms that include altered extracellular matrix composition and maturation. However, the role of ACE-011 in matrix mineralization will need to be examined further since the ash content of the L4 vertebrae was not altered in treated animals [20]. Follistatin was shown to play a role in bone development since mice deficient in follistatin are growth retarded, have abnormal tooth and craniofacial development and die within hours of delivery [32]. In addition, follistatin causes a dose-dependent blunting of BMP-induced osteoclastic bone resorption [33]. These results support our findings that ACE-011, which is systemically available and capable of binding to existing activin A, promotes bone formation by increasing osteoid thickness, mineral apposition rate, mineralizing surface, bone formation rate and osteoblast surface and decreases osteoclast surface, leading to increased cancellous bone mass. It should be noted that follistatin is known to regulate multiple ligands in the TGF- β family beyond activin A, including BMP-2, 4 and 7 which may also contribute to the osteoblast effects seen with follistatin deficiency.

The observed anabolic effects of ACE-011, an activin A antagonist, on the skeleton are in contrast to a previous report that activin A at low doses (1–5 μ g/kg) markedly increases vertebral bone mass and mechanical strength in aged OVX rats [34]. However, in the same study, a higher dosage of activin A (25 μ g/kg) diminishes the magnitude of these effects, providing evidence that the effects of activin on skeleton are dose-dependent. It therefore appears that the pharmacological blockade of activin signaling leads to increased bone mass in the present study.

Treatment with ACE-011 for 3 months had an inhibitory effect on cancellous bone resorption, suppressing osteoclast surface and eroded surface at distal femur and thoracic vertebra. Although a previous

Table 3
Effects of ACE-011 on cancellous bone microarchitecture of femoral neck.

Parameters	VEH	ACE-011
	(n = 4)	(n = 5)
BV/TV (%)	39.46 ± 3.05	47.23 ± 2.99
Tb.Th (μ m)	176 ± 7	193 ± 19
Tb.N (/mm)	2.54 ± 0.16	2.80 ± 0.23
Tb.Sp (μ m)	388 ± 29	308 ± 39
Conn.D (/mm ³)	18.85 ± 2.00	19.91 ± 4.22
SMI (–)	–0.13 ± 0.31	–1.20 ± 0.35*

Results are mean ± SEM. **p* < 0.05 compared to vehicle.

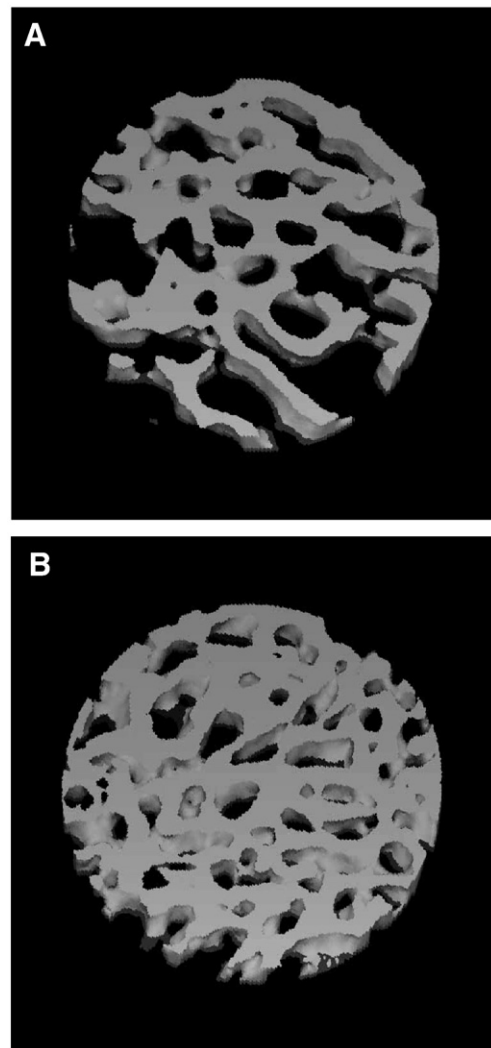


Fig. 3. Representative three-dimensional μ CT images showing more plate-like trabecular structure in ACE-011- (B) than VEH-treated monkeys (A).

study indicated that ActRIIA-mFc administration did not have any effect on bone resorption in OVX mice, it decreased osteoclast number and eroded surface after 2 weeks treatment in intact mice [19]. However, our findings are in agreement with those of Gaddy-Kurten et al. and others [18,35], who reported that activin A stimulates osteoclastogenesis *in vitro*. It has been shown that activin A stimulates I κ B- α , induces nuclear translocation of phosphorylated-NF κ B and increases RANK expression in osteoclast precursors [36]. The inhibitory effects of ACE-011 on bone resorption may be mediated, in part, by the ability of this compound to negatively regulate the actions of endogenous activin A and subsequently inhibit osteoclastogenesis. Although serum CTX, which measures systemic resorption, was not significantly altered, our histomorphometry data suggest that bone resorption might be decreased by ACE-011, at least in part, in cancellous bone. Indeed, the observed decreases in indices of cancellous bone resorption such as osteoclast surface and eroded surface in the distal femur and thoracic vertebra indicate that bone resorption was suppressed in monkeys treated with ACE-011.

Recently, a phase I clinical trial demonstrated that a single dose of ACE-011 caused a dose-dependent increase in serum levels of bone-specific ALP and dose-dependent decrease in CTX and TRACP 5b levels in postmenopausal women [22]. These results are consistent with our findings in monkeys that ACE-011 not only stimulates osteoblast formation, but also inhibits osteoclast resorption.

In conclusion, our results indicate that subcutaneous injection of soluble ActRIIA fusion protein ACE-011 for 3 months has no serious adverse effect. We detected significant changes in the bone anabolic effect of ACE-011 in Cynomolgus monkeys. Based on marked increases in osteoblast surface at distal femur and femoral neck, ACE-011 had a strong stimulatory effect on bone formation. In addition, ACE-011 served as antiresorptive agent at distal femur and thoracic vertebrae. These positive findings in non-human primate extend previous observations in rodents, and provide strong rationale for clinical investigation of ACE-011 for treatment of skeletal fragility.

Acknowledgments

The study was sponsored by Acceleron Pharma, Cambridge, MA. We thank Rajaram Manoharan for assistance with the μ CT imaging.

References

- Mulder JE, Kolatkar NS, LeBoff MS. Drug insight: existing and emerging therapies for osteoporosis. *Nat Clin Pract Endocrinol Metab* 2006;2:670–80.
- Neer RM, Arnaud CD, Zanchetta JR, Prince R, Gaich GA, Reginster JY, et al. Effect of parathyroid hormone (1–34) on fractures and bone mineral density in postmenopausal women with osteoporosis. *N Engl J Med* 2001;344:1434–41.
- Khosla S, Westendorf JJ, Oursler MJ. Building bone to reverse osteoporosis and repair fractures. *J Clin Invest* 2008;118:421–8.
- Massague J. The transforming growth factor- β family. *Annu Rev Cell Biol* 1990;6:597–641.
- Deli A, Kreidl E, Santifaller S, Trotter B, Seir K, Berger W, et al. Activins and activin antagonists in hepatocellular carcinoma. *World J Gastroenterol* 2008;14:1699–709.
- Pangas SA, Woodruff TK. Activin signal transduction pathways. *Trends Endocrinol Metab* 2000;11:309–14.
- Mathews LS. Activin receptors and cellular signaling by the receptor serine kinase family. *Endocr Rev* 1994;15:310–25.
- Hoodless PA, Wrana JL. Mechanism and function of signaling by the TGF β superfamily. *Curr Top Microbiol Immunol* 1998;228:235–72.
- Itoh S, Itoh F, Goumans MJ, Ten Dijke P. Signaling of transforming growth factor-beta family members through Smad proteins. *Eur J Biochem* 2000;267:6954–67.
- Matzuk MM, Kumar TR, Vassalli A, Bickenbach JR, Roop DR, Jaenisch R, et al. Functional analysis of activins during mammalian development. *Nature* 1995;374:354–6.
- Ogawa Y, Schmidt DK, Nathan RM, Armstrong RM, Miller KL, Sawamura SJ, et al. Bovine bone activin enhances bone morphogenetic protein-induced ectopic bone formation. *J Biol Chem* 1992;267:14233–7.
- Centrella M, McCarthy TL, Canalis E. Activin-A binding and biochemical effects in osteoblast-enriched cultures from fetal-rat parietal bone. *Mol Cell Biol* 1991;11:250–8.
- Sakai R, Miwa K, Eto Y. Local administration of activin promotes fracture healing in the rat fibula fracture model. *Bone* 1999;25:191–6.
- Oue Y, Kanatani H, Kiyoki M, Eto Y, Ogata E, Matsumoto T. Effect of local injection of activin A on bone formation in newborn rats. *Bone* 1994;15:361–6.
- Hashimoto M, Shoda A, Inoue S, Yamada R, Kondo T, Sakurai T, et al. Functional regulation of osteoblastic cells by the interaction of activin-A with follistatin. *J Biol Chem* 1992;267:4999–5004.
- Ikenoue T, Jingushi S, Urabe K, Okazaki K, Iwamoto Y. Inhibitory effects of activin-A on osteoblast differentiation during cultures of fetal rat calvarial cells. *J Cell Biochem* 1999;75:206–14.
- Eijken M, Swagemakers S, Koedam M, Steenbergen C, Derckx P, Uitterlinden AG, et al. The activin A-follistatin system: potent regulator of human extracellular matrix mineralization. *FASEB J* 2007;21:2949–60.
- Gaddy-Kurten D, Coker JK, Abe E, Jilka RL, Manolagas SC. Inhibin suppresses and activin stimulates osteoblastogenesis and osteoclastogenesis in murine bone marrow cultures. *Endocrinology* 2002;143:74–83.
- Pearsall RS, Canalis E, Cornwall-Brady M, Underwood KW, Haigis B, Ucran J, et al. A soluble activin type IIA receptor induces bone formation and improves skeletal integrity. *Proc Natl Acad Sci U S A* 2008;105:7082–7.
- Fajardo RJ, Manoharan RK, Pearsall RS, Davies MV, Marvell T, Monnell TE, Ucran JA, Pearsall AE, Khanzode D, Kumar R, Underwood KW, Roberts B, Seehra J, Bouxsein ML. Treatment with a soluble receptor for activin improves bone mass and structure in the axial and appendicular skeleton of female cynomolgus macaques (*Macaca fascicularis*). *Bone* 2010;46:64–71.
- Parfitt AM, Drezner MK, Glorieux FH, Kanis JA, Malluche H, Meunier PJ, et al. Bone histomorphometry: standardization of nomenclature, symbols, and units. Report of the ASBMR Histomorphometry Nomenclature Committee. *J Bone Miner Res* 1987;2:595–610.
- Ruckle J, Jacobs M, Kramer W, Pearsall AE, Kumar R, Underwood KW, et al. Single-dose, randomized, double-blind, placebo-controlled study of ACE-011 (ActRIIA-IgG1) in postmenopausal women. *J Bone Miner Res* 2009;24:744–52.
- Jerome CP, Johnson CS, Vafai HT, Kaplan KC, Bailey J, Capwell B, et al. Effect of treatment for 6 months with human parathyroid hormone (1–34) peptide in ovariectomized cynomolgus monkeys (*Macaca fascicularis*). *Bone* 1999;25:301–9.
- Smith SY, Dietrich J, Metcalfe A, MacLachlan R, Kimmel DB. Effects of rhPTH(1–84) on biochemical markers of bone turnover in the rhesus monkey. *J Bone Miner Res* 1997;12(Suppl 1):S237.
- Nakamura T, Takio K, Eto Y, Shibai H, Titani K, Sugino H. Activin-binding protein from rat ovary is follistatin. *Science* 1990;247:836–8.
- Menke DB, Page DC. Sexually dimorphic gene expression in the developing mouse gonad. *Gene Expr Patterns* 2002;2:359–67.
- de Kretser DM, Buzzard JJ, Okuma Y, O'Connor AE, Hayashi T, Lin SY, et al. The role of activin, follistatin and inhibin in testicular physiology. *Mol Cell Endocrinol* 2004;225:57–64.
- Tuuri T, Eramaa M, Hilden K, Ritvos O. The tissue distribution of activin beta A- and beta B-subunit and follistatin messenger ribonucleic acids suggests multiple sites of action for the activin-follistatin system during human development. *J Clin Endocrinol Metab* 1994;78:1521–4.
- Michel U, Rao A, Findlay JK. Rat follistatin: ontogeny of steady-state mRNA levels in different tissues predicts organ-specific functions. *Biochem Biophys Res Commun* 1991;180:223–30.
- Inoue S, Nomura S, Hosoi T, Ouchi Y, Orimo H, Muramatsu M. Localization of follistatin, an activin-binding protein, in bone tissues. *Calcif Tissue Int* 1994;55:395–7.
- Hashimoto MM, Shoda A, Inoue S, Yamada R, Kondo T, Sakurai T, et al. Functional regulation of osteoblastic cells by the interaction of activin-A with follistatin. *J Biol Chem* 1992;267:4999–5004.
- Matzuk MM, Lu N, Vogel H, Sellheyer K, Roop DR, Bradley A. Multiple defects and perinatal death in mice deficient in follistatin. *Nature* 1995;374:360–3.
- Kaneko H, Arakawa T, Mano H, Kaneda T, Ogasawara A, Nakagawa M, et al. Direct stimulation of osteoclastic bone resorption by bone morphogenetic protein (BMP)-2 and expression of BMP receptors in mature osteoclasts. *Bone* 2000;27:479–86.
- Sakai R, Fujita S, Horie T, Ohyama T, Miwa K, Maki T, et al. Activin increases bone mass and mechanical strength of lumbar vertebrae in aged ovariectomized rats. *Bone* 2000;27:91–6.
- Sakai R, Eto Y, Ohtsuka M, Hirafuji M, Shinoda H. Activin enhances osteoclast-like cell formation in vitro. *Biochem Biophys Res Commun* 1993;195:39–46.
- Sugatani T, Alvarez UM, Hruska KA. Activin A stimulates IkappaB-alpha/NFkappaB and RANK expression for osteoclast differentiation, but not AKT survival pathway in osteoclast precursors. *J Cell Biochem* 2003;90:59–67.